2011-07-21

Desorption Kinetics of an Alternative Monoethanolamine Based CO2 Capture Process

Morris D. Argyle
mdargyle@byu.edu

Zhuoyan Sun

Maohong Fan

Original Publication Citation

Z. Sun, M. Fan, M.D. Argyle, "Desorption Kinetics of the Monoethanolamine/Macroporous TiO2-Based CO2 Separation Process." Energy & Fuels, 25 2988-2996, 211.

Desorption kinetics of an alternative monoethenalamine based CO_2 capture process

Zhuoyan Sun,[§] Maohong Fan,[§,*] and Morris Argyle[§,ζ]

[§] *Department of Chemical & Petroleum Engineering, University of Wyoming, Laramie, WY 82071*

[ζ] *Department of Chemical Engineering, Brigham Young University, Provo, UT 84602*

ABSTRACT

Supported monoethenalamine (MEA) sorbents are promising materials for CO_2 separation due to their low energy demands. Like any other CO_2 separation technologies, CO_2 desorption from supported MEA sorbents is the most energy-expensive step in the overall CO_2 separation process. The presence of water during CO_2 desorption process leads to a significant increase in energy consumption. Therefore, CO_2 desorption in the absence of water is an important method to reduce energy consumption of CO_2 separation using supported MEA, which is determined by several major factors, including desorption kinetics. However, study on CO_2 desorption kinetics of supported MEA is lacking. This research was designed to make progress in this area. The CO_2 desorption kinetic model of TiO_2-supported MEA is experimentally derived with the data collected within water-free desorption environment and theoretically proved by pseudo-steady state theory. The Avrami–Erofeyev mechanism controls the CO_2 desorption process, which is first order with respect to [$RNH_3^+RNHCOO^-$] or RNH_3^+ or $RNHCOO^-$. The activation

*Corresponding author. E-mail: mfan@uwyo.edu.

energy of the CO_2 desorption process is 80.79 kJ/mol. The kinetic characteristics of the CO_2 desorption are much superior to those associated with aqueous MEA based CO_2 separation. The energy saving due to the use of supported MEA for CO_2 separation not only results from avoiding the use of water, with its high specific-heat capacity and high vaporization enthalpy, but also from the favorable desorption kinetics of the supported MEA based CO_2 separation.

INTRODUCTION

People are increasingly concerned about the continuous elevation of atmospheric CO_2 concentration. Fossil fuel based power generation plants have been and will continue to be among the major CO_2 emission sources due to their availability and prices.[1-4] Therefore, cost-effective technologies should be developed and adopted for capture of CO_2 from fossil fuel power plants while renewable or low-carbon-emission fuels are sought.[5, 6]

Amine compounds have been considered to be good candidates for CO_2 separation due to their good reactivity with CO_2.[7, 8] Monoethanolamine (MEA) has high potential as a CO_2 capture agent, since it has a high mass-based CO_2 sorption capacity and fast reaction rate with CO_2. CO_2 absorption with aqueous solutions can be expressed as

$$2RNH_2 + CO_2 + H_2O \xleftrightarrow{k_{R1},k_{-R1}} [RNH_3^+HCO_3^-]. \qquad (R1)$$

MEA has been commercially used for separation of CO_2 in the natural gas, synthesis gas, and refinery industries. However, to date, conventional coal-fired power plants still can not use aqueous MEA for CO_2 separation due to the high operating cost of the technology

resulting from its energy-intensive desorption process. In addition, thermal and oxidative degradations are issues of CO_2 separation with aqueous MEA, since CO_2 desorption needs to be operated within a relatively high temperature range, which leads to the loss of MEA during multiple sorption-desorption cycles.

To overcome the shortcomings of aqueous MEA based CO_2 separation processes, two major methods have been investigated. The first is to mix MEA with other amines to use their advantaages to overcome the shortcomings of MEA. For example, the CO_2 absorption rate can be enhanced significantly when MEA is blended with N-methyldiethanolamine (MDEA), while the associated CO_2 desorption is improved.[9, 10] However, these CO_2 sorption systems are still aqueous-phase. People have been interested in this type of method for a long time; thus, the thermodynamic and kinetic characteristics of CO_2 separation with blended aqueous amines have been well studied.[11-16] The second method is to replace water with organic solvents. Jou et al. found that diethylene glycol (DEG) can dissolve much more CO_2 than water.[17] Glycol compounds, including ethylene glycol (EG), DEG, and triethylene glycol (TEG), have shown high CO_2 solubility and low vapor pressure, which is desired for reducing the total energy consumption needed for overall CO_2 separation process.[18] Essentially, replacing water with organic solvents is used to eliminate the dissociation of protonated MEA or formation of carbonate or carbamate within the aqueous environment or recombination of water and MEA, and thus reduce energy consumption.[19]

Recently, researchers have been very interested in developing solid CO_2 sorbents with various amines, making significant progress in increasing CO_2 sorption capacities and lowering CO_2 desorption temperatures.[20-28] When used for separation of CO_2 from

flue gases in power plants, they could save much energy by avoiding circulation of large amounts of water. One of the methods used for preparing those solid sorbents is to physically impregnate amines, including MEA,[20, 29, 30] onto the surfaces of porous supporting materials.

Recently, this research team has developed an alternative, semi-immobilization method for preparing supported MEA sorbent. Specifically, pure MEA is immobilized during the CO_2 sorption process, but is mobilized during the CO_2 desorption phase. In other words, immobilized pure MEA reacts with CO_2 in one sorption rector, and then is transferred to another reactor during the CO_2 desorption process through vaporization. In the absence of water, the MEA based CO_2 separation process can be written as

$$2RNH_2 + CO_2 \xleftrightarrow{k_{R2},k_{-R2}} [RNH_3^+RNHCOO^-]. \qquad (R2)$$

The alternative MEA application method is designed to use the advantages of solid sorbents while avoiding their hydrothermal/steam stability issues.[28] It could be used to further reduce the energy needed for MEA-based CO_2 separation technologies. As mentioned earlier, desorption step is the key process for any CO_2 separation technology. Therefore, understanding the kinetics of CO_2 desorption in R2 is important to the development of the technology. However, the study on the kinetics of CO_2 desorption of R2, in the absence of water, is lacking. Thus, this research was focused on building a kinetic model for CO_2 desorption in R2 (the reverse reaction of R2, designated as -R2).

EXPERIMENTAL SECTION

TiO_2 preparation and characterization and sorbent preparation

The TiO_2 used as a support for MEA in this research was prepared with $Ti(OC_2H_5)_4$ (99 wt%, Acros) through several steps. The first was to add the needed quantity of $Ti(OC_2H_5)_4$ to water with the H_2O:$Ti(OC_2H_5)_4$ molar ratio being 26.3. Next, the mixture was stirred for 1 hr. Then, the obtained precipitate, $[TiO(OH)_2]$, was filtered, washed with deionized water, and dried at 393K for ~1.5 hrs. TiO_2 was made after calcining the $TiO(OH)_2$ at 1023K in flowing air for 3 hours.

The prepared TiO_2 was characterized using a Micromeritics TriStar 3000 V6.04 A nitrogen physisorption analyzer to determine its surface area by the BET (Brunauer, Emmett, and Teller) method. The morphological characteristics of this MEA supporting material (TiO_2) were analyzed using a Hitachi TM-1000 tabletop scanning electron microscope (SEM).

MEA-TiO_2 (MT) sorbent was made by mixing a defined amount of as-received MEA (99 wt%, Acros) with the prepared TiO_2. The mass ratio of MEA:TiO_2 used for the sorption tests in this research was 40:60.

Apparatus and CO_2 sorption/desorption

The experimental apparatus constructed for this research is shown in Figure 1. It consists of three parts, including a gas simulation unit, a CO_2 sorption/desorption system, and CO_2 on-line measurement equipment. Dilute CO_2 from cylinder 1 (1 vol% CO_2 and 99 vol% N_2) was used for the sorption tests while N_2 from cylinder 2 (100 vol%) was used during CO_2 desorption and the apparatus cleaning process. The flow rates of the two inlet gases were controlled by their corresponding flow meters (Matheson Tri-gas FM-

1050, numbed as 3' and 3''). Another flow meter (3''') was placed to measure the flow of the whole system.

This research focused on studying the kinetics of CO_2 desorption in a water-free environment. The sorption performance of the MT will be reported separately. For the present work, the purpose of doing sorption tests was to generate the spent sorbents used for the CO_2 desorption kinetic study. Sorption tests were performed in the reactor (#8 in Figure 1, 9 mm x 610 mm). The sorbent bed (#6) was made by loading MT sorbent between two bed holders (#5) made from quartz wool. The reactor (#8) was held in a tube furnace (#7, Thermo Corporation, TF55030A-1) whose temperature was adjusted by a temperature controller (#4, Yokogawa M&C Corporation, UT150). The effluent gas from the reactor (#8) entered a water removal unit (#10) and then an infrared gas analyzer (#11, ZRE, Fuji Electric System Co. Ltd.). The sorption profiles were collected by a data collection computer (#12). All the sorption tests were done under the following conditions: 1.0 vol% CO_2; 99.0 vol% N_2; 0.3 L/min gas flow rate, and 40°C sorption temperature. Each sorption test was stopped when the CO_2 concentration in outlet gas was the same as the initial CO_2 concentration (1.0 vol%).

Desorption tests were performed to study the kinetics of CO_2 desorption in R2 (-R2). The first step of the CO_2 desorption operation was to load the spent MT generated during sorption step into the reactor (#8). All the desorption tests were performed with pure N_2 from cylinder 2 as a carrier gas with a flow rate of 0.3 L/min. The initial amount of $[RNH_3^+RNHCOO^-]$ in the spent sorbent used for each CO_2 desorption was obtained by integrating the corresponding CO_2 sorption or desorption profiles. During the desorption process, the MEA and CO_2 decomposed from $[RNH_3^+RNHCOO^-]$ passed through a MEA

removal bottle (#10) loaded with 1.0 M H_2SO_4 solution. The MEA-stripped gas from the bottle passed through the gas analyzer (#11) for CO_2 concentration measurement. CO_2 desorption tests were done at five temperatures to obtain the Arrhenius form of -R2.

3. Results and Discussion

3.1 Characteristics of TiO_2

The BET surface area, average pore size, and volume of the TiO_2 as the supporting material of the MT sorbent are 5.68 m^2/g, 66.4 nm, and 0.11 cm^3/g, respectively. A typical SEM image of the TiO_2 is shown in Figure 2, indicating that the TiO_2 is porous and has a well developed network structure.

3.2 CO_2 desorption kinetic model obtained by experiment

Theory

Essentially, CO_2 desorption, or spent sorbent [$RNH_3^+RNHCOO^-$] decomposition (-R2), is the reverse reaction of R2. Under isothermal conditions, the experimental set-up shown in Figure 1 was used to study the kinetics of CO_2 desorption from or thermal decomposition of the spent sorbent [$RNH_3^+RNHCOO^-$] obtained through the sorption of CO_2 with pure MEA. Like the thermal decomposition processes of many other compounds, [31-36] the general thermal decomposition model of [$RNH_3^+RNHCOO^-$], or CO_2 desorption, can be represented with the following equation

$$F(\alpha) = \mathrm{kt} \qquad \text{(E1)}$$

where k is the rate coefficient of -R2, or CO_2 desorption, and *t* is the reaction time of -R2, F(α) is the function of α, the mass fraction of decomposed [$(RNH_3)^+(RNHCOO)^-$] at any reaction time (*t*).

The specific definition of α in E1 of -R2 is expressed as

$$\alpha = \frac{W_{[RNH_3^+RNHCOO^-]_0} - W_{[RNH_3^+RNHCOO^-]_t}}{W_{[RNH_3^+RNHCOO^-]_0}} = \frac{\Delta W_{[RNH_3^+RNHCOO^-]_t}}{W_{[RNH_3^+RNHCOO^-]_0}} \quad \text{(E2)}$$

where $W_{[RNH_3^+RNHCOO^-]_0}$ is the initial mass (g) of [$RNH_3^+RNHCOO^-$], $W_{[RNH_3^+RNHCOO^-]_t}$ is the mass (g) of [$RNH_3^+RNHCOO^-$] at any CO_2 desorption or [$RNH_3^+RNHCOO^-$] decomposition time, *t*, $\Delta W_{[RNH_3^+RNHCOO^-]_t}$ is the decomposed [$RNH_3^+RNHCOO^-$] at *t*. Both $W_{[RNH_3^+RNHCOO^-]_0}$ and $W_{[RNH_3^+RNHCOO^-]_t}$ can be calculated by integration since 1 mole of desorbed CO_2 results from the decomposition of 1 mole of [$RNH_3^+RNHCOO^-$], according to R2. $W_{[(RNH_3)^+(RNHCOO)^-]_0}$ can be obtained by using both CO_2 sorption and the corresponding desorption profiles of [$RNH_3^+RNHCOO^-$] formed during sorption step. Typical profiles of CO_2 sorption with MEA and CO_2 desorption from [$RNH_3^+RNHCOO^-$] are presented in Figures 3 and 4, respectively. [$RNH_3^+RNHCOO^-$] was completely decomposed into RNH_2 and CO_2 at 80°C. In other words, the spent sorbent is totally regenerable at 80°C. The values of α should change from 0 to 1 from the beginning to the end of [$RNH_3^+RNHCOO^-$] decomposition. Based on the CO_2 desorption profiles collected with the gas analyzer at different temperatures, the corresponding α vs *t* relationships were calculated.

F(α) can be represented by different kinetic expressions, although only one of them should fit a specific reaction best. The seven major functional representations of F(α)[32] include α^2 , $\alpha+(1-\alpha)\ln(1-\alpha)$, $[1-(1-\alpha)^{1/3}]^2$, $1-\frac{2}{3}\alpha-(1-\alpha)^{2/3}$, $\ln[\alpha/(1-\alpha)]$, $1-(1-\alpha)^{1/n}$, and $-\ln(1-\alpha)^{1/m}$.

However, the most frequently used forms of F(α) are

$$F(\alpha) = 1-(1-\alpha)^{1/n} \qquad (n = 1, 2, \text{and } 3) \qquad (E3)$$

$$F(\alpha) = -\ln(1-\alpha)^{1/m} \qquad (m = 1, 1.5, 2, 3, \text{and } 4). \qquad (E4)$$

They have been successfully used by researchers to study the kinetics of many chemical processes, especially those associated with decomposition of chemical compounds.[31-37] For example, Marinoni et al.[31] found that E4 (also called Avrami–Erofeyev equation) can well represent the kinetics of mullitization in a porcelain-like precursor system. Tang et al. found that E3 applied to the kinetics of thermal dehydration of $CaCO_3{\cdot}H_2O$.[32] Koga confirmed that E3 and E4 apply separately for the thermal dehydration of α-nickel sulfate hexahydrate under different conditions.[33] Furthermore, the Avrami–Erofeyev equation can be used for modeling the kinetic data Konieczny et al. collected when they studied methane decomposition reactions catalyzed by iron based catalysts for hydrogen production.[34]

Experimentally derived rate equation and Arrhenius form of CO_2 desorption

The CO_2 desorption (-R2) studied in this research is a typical decomposition reaction. Therefore, all of the aforementioned seven F(α) forms were tested against preliminary experimental results for their relationships with *t*, as shown in E1. The

derived regression coefficients indicated that E3 and E4 deserved more evaluation since they resulted in higher regression coefficients. Thus, E3 and E4 were chosen for further comparative studies. The values of the CO_2 desorption reaction order (n and m), CO_2 desorption rate coefficient (k), and corresponding correlation coefficient (r^2) obtained at different temperatures of the two models are listed in Table 1.

Table 1 shows that the regression coefficients of both models at all the sorption temperatures are high; however, the obtained reaction orders (n) in $F(\alpha) = 1-(1-\alpha)^{1/n}$ vary considerably within the temperature range. Therefore, Avrami–Erofeyev equation (E4) represents the CO_2 desorption mechanism of -R2 better than E3 does. All five of the $-\ln(1-\alpha)^{1/m}$ versus t plots obtained at 45°C, 52°C, 66°C, 70°C and 73°C are shown in Figure 5. The average reaction order at the five desorption temperatures is 1.21. Therefore, the reaction order of CO_2 desorption with respect to [$RNH_3^+RNHCOO^-$] can be considered to be approximately 1. Thus, the rate equation of CO_2 desorption without presence of water (-R2) is

$$\frac{d\alpha}{dt} = k(1-\alpha)\,. \qquad \text{(E5)}$$

Figure 6 compares this first order model with the experimental data for $F(\alpha)$ vs t. The model produces an excellent fit for the data when m = 1.09, which further reinforces how closely the reaction order can be approximated as unity.

The relationship between rate constants (k) of -R2 listed in Table 1 and the corresponding CO_2 desorption temperature (T) can be correlated by the Arrhenius equation[38]

$$k = Ae^{-\frac{E}{RT}} \qquad \text{(E6)}$$

where *A* is the pre-exponential factor (min^{-1}), which is treated as a constant in the studied temperature range; *E* is the activation energy (J/mol) of CO_2 desorption in the absence of water; and R is the ideal gas constant (J/mol·K).

The $\ln k \sim \frac{1}{T}$ plot for CO_2 desorption, based on the values of k at 45°C, 52°C, 59°C, 66°C, and 73°C, is shown in Figure 7. An E value of 80.79 kJ/mol and an A value of 4.2999×10^{11} (min^{-1}), respectively, were regressed. Therefore, the Arrhenius form of CO_2 desorption from [$RNH_3^+RNHCOO^-$] is

$$k = 4.2999\times10^{11} e^{-\frac{8.079\times10^4}{RT}} \quad \text{(E7)}$$

3.3 CO_2 desorption kinetic model derived from pseudo-steady state theory

Integrating pseudo-steady state theory with the studied CO_2 desorption

CO_2 sorption and desorption without the presence of water proceeds through the following steps, based on the theory of CO_2 sorption with MEA[39, 40]

$$CO_2 + RNH_2 \xleftarrow{k_{R3},k_{-R3},K_{R3}} RNH_2^+COO^- \quad \text{(R3)}$$

$$RNH_2^+COO^- + RNH_2 \xleftarrow{k_{R4},k_{-R4},K_{R4}} RNH_3^+RNHCOO^- . \quad \text{(R4)}$$

$RNH_2^+COO^-$ is the intermediate species. Then, according to pseudo-steady state theory, the generation and consumption rates of $RNH_2^+COO^-$ in R3 and R4 should be equal, or

$$\begin{aligned}\frac{d[RNH_2^+COO^-]}{dt} &= k_{R3}[CO_2][RNH_2] - k_{-R3}[RNH_2^+COO^-] \\ &\quad - k_{R4}[RNH_2^+COO^-][RNH_2] + k_{-R4}[RNH_3^+RNHCOO^-] \\ &= 0\end{aligned} \quad \text{(E8)}$$

or

$$\left[RNH_2^+COO^-\right] = \frac{k_{R3}[CO_2][RNH_2] + k_{-R4}[RNH_3^+RNCHCOO^-]}{k_{-R3} + k_{R4}[RNH_2]}. \quad \text{(E9)}$$

Based on the rate law, the change of $[RNH_3^+RNHCOO^-]$ with time (t) can be expressed in terms of conversion fraction (α) as

$$M_0 \frac{d\alpha}{dt} = -\frac{d[RNH_3^+RNHCOO^-]}{dt}$$
$$= k_{-R4}[RNH_3^+RNHCOO^-] - k_{R4}[RNH_2][RNH_2^+COO] \quad \text{(E10)}$$

where M_0 is the initial concentration of $[RNH_3^+RNHCOO^-]$. Combining E9 and E10 leads to

$$M_0 \frac{d\alpha}{dt} = k_{-R4}\left[RNH_3^+RNHCOO^-\right]$$
$$- k_{R4}[RNH_2]\frac{k_{R3}[CO_2][RNH_2] + k_{-R4}[RNH_3^+RNCHCOO^-]}{k_{-R3} + k_{R4}[RNH_2]}. \quad \text{(E11)}$$

Based on the stoichiometry of R2, when αM_0 of $[RNH_3^+RNHCOO^-]$ is consumed at time, t, the concentrations of $[RNH_3^+RNHCOO^-]$, $[RNH_2]$ and $[CO_2]$ at that moment should be

$$[RNH_3^+RNHCOO^-] = (1-\alpha)M_0 \quad \text{(E12)}$$

$$[RNH_2] = 2\alpha M_0 \quad \text{(E13)}$$

$$[CO_2] = \alpha M_0 \quad \text{(E14)}$$

respectively. Integrating E11, E12, E13, and E14 results in

$$M_0 \frac{d\alpha}{dt} = \frac{k_{-R3}k_{-R4}[1-\alpha]M_0 - 4k_{R3}k_{R4}\alpha^3 M_0^3}{k_{-R3} + 2k_{R4}\alpha M_0} \quad \text{(E15)}$$

or

$$\frac{d\alpha}{dt} = \frac{k_{-R3}k_{-R4}[1-\alpha]-4k_{R3}k_{R4}\alpha^3 M_0^2}{k_{-R3}+2k_{R4}\alpha M_0} \quad \text{(E16)}$$

.

During the $[RNH_3^+RNHCOO^-]$ decomposition or CO_2 desorption period, k_{-R4} and k_{-R5} are much larger than k_{R4} and k_{R5}, respectively; therefore, E16 can be simplified as

$$\frac{d\alpha}{dt} = k_{-R4}[1-\alpha] = k[1-\alpha] \quad \text{(E17)}$$

or

$$-\frac{d[1-\alpha]M_0}{dt} = -\frac{d[RNH_3^+RNHCOO^-]}{dt} = k[1-\alpha]M_0 \quad \text{(E18)}$$

or

$$r_{CO_2\text{-desorption}} = -\frac{d[RNH_3^+RNHCOO^-]}{dt} = k[RNH_3^+RNHCOO^-] \quad \text{(E19)}$$

.

In other words, the CO_2 desorption or $[RNH_3^+RNHCOO^-]$ decomposition rate is 1st order with respect $[RNH_3^+RNHCOO^-]$, which is consistent with that derived with Avrami-Erofeyev mechanism and the experimental data, as discussed earlier.

Activity based rate equation

According to the thermodynamic definition of activity (*a*), $a_{[RNH_3^+RNHCOO^-]}$ is related to $a_{[RNH_3^+]}$ and $a_{[RNHCOO^-]}$ as follows

$$a_{[RNH_3^+RNHCOO^-]} = a_{[RNH_3^+]}a_{[RNHCOO^-]}. \quad \text{(E20)}$$

or

$$\gamma_{[RNH_3^+RNHCOO^-]}[RNH_3^+RNHCOO^-] = \gamma_{[RNH_3^+]}[RNH_3^+]\gamma_{[RNHCOO^-]}[RNHCOO^-] \quad \text{(E21)}$$

where γ_i {i = [$RNH_3^+RNHCOO^-$], RNH_3^+, $RNHCOO^-$} is the activity coefficient of species, *i*. Assuming

$$\gamma_{[RNH_3^+RNHCOO^-]} = \gamma_{[RNH_3^+]} = \gamma_{[RNHCOO^-]} = 1, \quad \text{(E22)}$$

then, combining E19 through E22 leads to

$$\begin{aligned} r_{CO_2\text{-desorption}} &= k a_{RNH_3^+} a_{RNHCOO^-} \\ &= 4.2999\times10^{11} e^{-\frac{8.0795\times10^4}{RT}} a_{RNH_3^+} a_{RNHCOO^-} \end{aligned} \quad \text{(E23)}$$

The reaction orders with respect to the two species, RNH_3^+ and $RNHCOO^-$, in $[RNH_3^+RNHCOO^-]$ are both 1. E23 shows that the CO_2 desorption rate is proportional to the product of the activities of RNH_3^+ and $RNHCOO^-$.

3.4 Effect of water on CO_2 desorption kinetics

The sorption kinetics of CO_2 separations with aqueous MEA solutions have been extensively studied,[41-45] although more work needs to be done to study their desorption kinetics. However, to the knowledge of this research team, little research has been performed on the kinetics of CO_2 separation with MEA in absence of water. Plaza et al.[46] studied the kinetics of CO_2 desorption under conditions of aqueous and highly concentrated MEA solutions.[47] All major kinetic parameters of their models are listed in Table 2. The CO_2 desorption reaction orders with respect to RNH_3^+ and $RNHCOO^-$ within highly concentrated MEA solutions shown in Table 2 are exactly the same as those this research team obtained as given in E23. Comparison of Table 2 with E7/E23 also indicates that the activation energy values of CO_2 desorption are different under the

three sorption and desorption conditions: aqueous, highly concentrated MEA, and a water-free environment.

Desorption reaction order

Table 2 shows that water plays a negative role in CO_2 desorption within an aqueous environment. The rate of the reverse reaction of R1, or CO_2 desorption, is inversely proportional to the activity of water. In other words, lower water activity within MEA-based CO_2 separation systems is beneficial to CO_2 desorption.

Understanding the effect of water on CO_2 desorption kinetics can start with that on CO_2 sorption kinetics. Water affects the overall CO_2 sorption kinetics of aqueous MEA based CO_2 separation,[39, 40, 45, 48-50] although the degree of influence needs further investigation because scientists have some disagreement on this subject.[45] Water affects CO_2 sorption in aqueous or even highly concentrated MEA solutions in different ways. The first one is its own dissociation:

$$2H_2O \leftrightarrow OH^- + H_3O^+. \qquad \text{(R5)}$$

The active hydroxyl ion, OH^-, resulting from R5 can directly react with CO_2 to form bicarbonate

$$OH^- + CO_2 \leftrightarrow HCO_3^-. \qquad \text{(R6)}$$

The rate equation of R6 has been found to be

$$-\frac{d[OH^-]}{dt} = k_{R6}[CO_2][OH^-] \qquad \text{(E24)}$$

where k_{R6} [m^3/(kmol·s)] is the specific reaction rate with respect to [OH^-].[51-53] The Arrhenius form of R6[51-53] is

$$k_{R6} = 4.48 \times 10^{13} e^{-\frac{5.5429 \times 10^4}{RT}} \quad . \qquad \text{(E25)}$$

The low activation energy and high pre-exponential factor in E25 indicate R6 is a fast reaction. Next, H_2O molecules can also directly interact with CO_3^{2-} to form hydroxyl ions (OH^-) through the following reaction

$$CO_3^{2-} + H_2O \leftrightarrow HCO_3^- + OH^- . \qquad \text{(R7)}$$

R6 and R7 indicate that H_2O positively affects CO_2 sorption. Moreover, H_2O can react with $RNH_2^+COO^-$, $RNHCOO^-$, and RNH_3^+ resulting from the overall MEA sorption process. It also plays a positive role in CO_2 sorption through these reactions.[45, 48, 52] Therefore, the overall CO_2 sorption rate should be affected positively to some degree by the activity of H_2O (a_{H_2O}),[45] which leads to conclusion that water negatively affects CO_2 desorption, since all the reaction steps involved with H_2O are reversible and H_2O is present as a reactant there. This is confirmed by the negative reaction order (-1) of CO_2 desorption with respect to H_2O in the aqueous H_2O-CO_2 system, as shown in Table 2

Furthermore, a_{H_2O} is not only affected by the concentration of water, but also by that of $RNH_3^+HCO_3^-$ formed within the aqueous H_2O-CO_2 environment according to Blandamer et al.[54] The value of a_{H_2O} is related to the molality of $RNH_3^+HCO_3^-$ and other parameters as follows[54, 55]

$$\ln a_{H_2O} = -2M_{H_2O} m_{RNH_3^+HCO_3^-} + 2(S_\gamma / 3) M_{H_2O} (m^o)^{-\frac{1}{2}} (m_{RNH_3^+HCO_3^-})^{\frac{3}{2}} \qquad \text{(E27)}$$

where M = 0.018 kg·mol^{-1}, $m_{RNH_3^+HCO_3^-}$ is the molality of $RNH_3^+HCO_3^-$, m^o = 1 mol·kg^{-1}, and S_γ is defined as

$$S_\gamma = \frac{e^3[2N_A\rho_{H_2O}m^o]^{\frac{1}{2}}}{8\pi[\varepsilon_0\varepsilon_r kT]^{\frac{3}{2}}} \quad \text{(E28)}$$

where e = 2.718, N_A = Avogadro's number, ρ_{H_2O} is the density of water, ε_0 is the permittivity of vacuum, ε_r is the relative permittivity of H_2O, and k is Boltzmann's constant. E27 and E28 indicate that a_{H_2O} is increased or CO_2 desorption rate decreases according to Plaza et al.[46] in an aqueous MEA-based CO_2 sorption system.

Desorption activation energy

The activation energy values of CO_2 desorption decrease from ~114 kJ/mol to ~103 kJ/mol when the CO_2 sorption environment changes from an aqueous to a highly concentrated MEA solution. Furthermore, the activation energy obtained with this research within a completely nonaqueous CO_2 sorption-desorption system is ~81 kJ/mol. The ~20% activation energy difference between our and Plaza's reported activation energies can be attributed to the difference in the experimental conditions under which CO_2 desorption data were collected and upon which the corresponding kinetic models were built. Plaza's CO_2 desorption model[46] for R2 was based on data from CO_2 sorption and desorption experiments performed with concentrated MEA which still contained water, unlike the pure MEA used in this research. The information provided from comparison of the three activation energy values obtained from the different conditions (aqueous MEA, highly concentrated MEA, and water-free MEA) is that the presence of water leads to the increase of activation energy of the CO_2 desorption reaction.

Conclusion

The CO_2 desorption kinetic model for CO_2 separation using TiO_2-supported MEA is different from those using aqueous MEA and highly concentrated MEA solutions. Separation of CO_2 with supported but semi-immobilized pure MEA could significantly reduce energy consumption compared to conventional aqueous MEA, not only due to the elimination of the use of a large amount of water with its high specific-heat-capacity and latent heat of vaporization, but also the improvement of CO_2 desorption kinetics resulting from avoiding dissociation of the protonated MEA.

The findings in this CO_2 desorption kinetic research are not only of importance to the economics of MEA-based CO_2 separation technologies, but also to its environmental considerations. Improvement in CO_2 desorption kinetics through use of supported but semi-immobilized pure MEA implies that lower temperatures can be used for CO_2 desorption, which can alleviate the thermal and oxidative degradation problems observed in aqueous MEA-CO_2 separation system. In addition, lower CO_2 sorption temperatures can help coal-fired power plants mitigate the corrosion issues associated with aqueous MEA-CO_2 separation systems. Decreased corrosion can result in a decrease in the amount of iron carbonate particles in the MEA-CO_2 reaction system, avoiding operational difficulties that include foaming, emulsions, and fouling of aqueous systems, and thus improve the stability and reliability of CO_2 separation facilities in terms of operation, CO_2 sorption capacity, and MEA regeneration ability.

Reference

1. Quick, J. C., *Environ. Sci. Technol.* **2010,** *44* (7), 2709-2714.
2. O'Keefe, J. M. K.; Henke, K. R.; Hower, J. C.; Engle, M. A.; Stracher, G. B.; Stucker, J. D.; Drew, J. W.; Staggs, W. D.; Murray, T. M.; Hammond, M. L.; Adkins, K. D.; Mullins, B. J.; Lemley, E. W., *Sci. Total Environ.* **2010,** *408* (7), 1628-1633.
3. Chiao, C.-H.; Chen, J.-L.; Lan, C.-R.; Chen, S.; Hsu, H.-W., *Sustainable Environment Research* **2011,** *21* (1), 1-8.
4. Notz, R.; Toennies, I.; McCann, N.; Scheffknecht, G.; Hasse, H., *Chem. Eng. Technol.* **2011,** *34* (2), 163-172.
5. McIlveen-Wright, D. R.; Huang, Y.; Rezvani, S.; Mondol, J. D.; Redpath, D.; Anderson, M.; Hewitt, N. J.; Williams, B. C., *Fuel* **2011,** *90* (1), 11-18.
6. Hossain, A. K.; Davies, P. A., *Renewable Energy* **2010,** *35* (1), 1-13.
7. Porcheron, F.; Gibert, A.; Mougin, P.; Wender, A., *Environ. Sci. Technol.* **2011,** *45* (6), 2486-2492.
8. Puxty, G.; Rowland, R., *Environ. Sci. Technol.* **2011,** *45* (6), 2398-2405.
9. Lawal, A. O.; Idem, R. O., *Ind. Eng. Chem. Res.* **2006,** *45* (8), 2601-2607.
10. Lawal, O.; Bello, A.; Idem, R., *Ind. Eng. Chem. Res.* **2005,** *44* (6), 1874-1896.
11. Ho, M. T.; Allinson, G. W.; Wiley, D. E., *Int. J. Greenhouse Gas Control* **2011,** *5* (1), 49-60.
12. Cui, Z.; Aroonwilas, A.; Veawab, A., *Ind. Eng. Chem. Res.* **2010,** *49* (24), 12576-12586.
13. Simons, K.; Brilman, W.; Mengers, H.; Nijmeijer, K.; Wessling, M., *Ind. Eng. Chem. Res.* **2010,** *49* (20), 9693-9702.
14. Mangalapally, H. P.; Notz, R.; Hoch, S.; Asprion, N.; Sieder, G.; Garcia, H.; Hasse, H., *Energy Procedia* **2009,** *1* (1), 963-970.
15. Godini, H. R.; Mowla, D., *Chem. Eng. Res. Des.* **2008,** *86* (4), 401-409.

16. Abu-Zahra, M. R. M.; Niederer, J. P. M.; Feron, P. H. M.; Versteeg, G. F., *Int. J. Greenhouse Gas Control* **2007,** *1* (2), 135-142.

17. Jou, F. Y.; Otto, F. D.; Mather, A. E., *Fluid Phase Equilib.* **2000,** *175* (1-2), 53-61.

18. Wu, H.; Chung, T. W., *Ind. Eng. Chem. Res.* **2008,** *47* (19), 7397-7404.

19. Tan, J.; Shao, H.-W.; Xu, J.-H.; Du, L.; Luo, G.-S., *Ind. Eng. Chem. Res.* **2011**.

20. Ma, X. L.; Wang, X. X.; Song, C. S., *J. Am. Chem. Soc.* **2009,** *131* (16), 5777-5783.

21. Son, W. J.; Choi, J. S.; Ahn, W. S., *Microporous Mesoporous Mater.* **2008,** *113* (1-3), 31-40.

22. Yue, M. B.; Sun, L. B.; Cao, Y.; Wang, Z. J.; Wang, Y.; Yu, Q.; Zhu, J. H., *Microporous Mesoporous Mater.* **2008,** *114* (1-3), 74-81.

23. Tsuda, T.; Fujiwara, T., *J. Chem. Soc., Chem. Commun.* **1992,** (22), 1659-1661.

24. Gray, M. L.; Soong, Y.; Champagne, K. J.; Pennline, H.; Baltrus, J. P.; Stevens, R. W.; Khatri, R.; Chuang, S. S. C.; Filburn, T., *Fuel Process. Technol.* **2005,** *86* (14-15), 1449-1455.

25. Zelenak, V.; Halamova, D.; Gaberova, L.; Bloch, E.; Llewellyn, P., *Microporous Mesoporous Mater.* **2008,** *116* (1-3), 358-364.

26. Hicks, J. C.; Drese, J. H.; Fauth, D. J.; Gray, M. L.; Qi, G. G.; Jones, C. W., *J. Am. Chem. Soc.* **2008,** *130* (10), 2902-2903.

27. Choi, S.; Drese, J. H.; Eisenberger, P. M.; Jones, C. W., *Environ. Sci. Technol.* **2011,** *45* (6), 2420-2427.

28. Li, W.; Bollini, P.; Didas, S. A.; Choi, S.; Drese, J. H.; Jones, C. W., *ACS Appl. Mater. Interfaces* **2010,** *2* (11), 3363-3372.

29. Hogendoorn, J. A.; Van Swaaij, W. P. M.; Versteeg, G. F., *Chem. Eng. Commun.* **1996,** *144*, 19-50.

30. Filburn, T.; Helble, J. J.; Weiss, R. A., *Ind. Eng. Chem. Res.* **2005,** *44* (5), 1542-1546.

31. Marinoni, N.; Pagani, A.; Adamo, I.; Diella, V.; Pavese, A.; Francescon, F., *J. Eur. Ceram. Soc.* **2011,** *31* (3), 273-280.

32. Tang, W. J.; Chen, D. H.; Wang, C. X., *AlChE J.* **2006,** *52* (6), 2211-2216.

33. Koga, N.; Tanaka, H., *J. Phys. Chem.* **1994,** *98* (41), 10521-10528.

34. Konieczny, A.; Mondal, K.; Wiltowski, T.; Dydo, P., *Int. J. Hydrogen Energy* **2008,** *33* (1), 264-272.

35. Tanaka, H.; Ohshima, S.; Ichiba, S.; Negita, H., *Thermochim. Acta* **1981,** *48* (1-2), 137-146.

36. Koradia, V.; de Diego, H. L.; Elema, M. R.; Rantanen, J., *J. Pharm. Sci.* **2010,** *99* (9), 3966-3976.

37. Halasz, I.; Mestrovic, E.; Cicak, H.; Mihalic, Z.; Vancik, H., *J. Org. Chem.* **2005,** *70* (21), 8461-8467.

38. Fogler, H. S., *Elements of Chemical Reaction Engineering.* 4 ed.; Prentice Hall PTR: 2006.

39. Aboudheir, A.; Tontiwachwuthikul, P.; Chakma, A.; Idem, R., *Chem. Eng. Sci.* **2003,** *58* (23-24), 5195-5210.

40. Han, B.; Zhou, C.; Wu, J.; Tempel, D. J.; Cheng, H., *Phys. Chem. Lett.* **2011,** *2*, 522–526.

41. Usubharatana, P.; Tontiwachwuthikul, P., *Energy Procedia* **2009,** *1* (1), 95-102.

42. Zhang, Y.; Chen, H.; Chen, C. C.; Plaza, J. M.; Dugas, R.; Rochelle, G. T., *Ind. Eng. Chem. Res.* **2009,** *48* (20), 9233-9246.

43. Edali, M.; Aboudheir, A.; Idem, R., *Int. J. Greenhouse Gas Control* **2009,** *3* (5), 550-560.

44. Jamal, A.; Meisen, A.; Lim, C. J., *Chem. Eng. Sci.* **2006,** *61* (19), 6590-6603.

45. Ramachandran, N.; Aboudheir, A.; Idem, R.; Tontiwachwuthikul, P., *Ind. Eng. Chem. Res.* **2006,** *45* (8), 2608-2616.

46. Plaza, J. M.; Van Wagener, D.; Rochelle, G. T., *Int. J. Greenhouse Gas Control* **2010,** *4* (2), 161-166.

47. Aboudheir, A. A. Kinetics, modeling, and simulation of carbon dioxide absorption into highly concentrated and loaded monoethanolamine solutions. Univ. of Regina, Regina, 2002.

48. Glasscock, D. A.; Critchfield, J. E.; Rochelle, G. T., *Chem. Eng. Sci.* **1991,** *46* (11), 2829-2845.

49. Dugas, R.; Rochelle, G., *Energy Procedia* **2009,** *1* (1), 1163-1169.

50. Abu-Zahra, M. R. M.; Schneiders, L. H. J.; Niederer, J. P. M.; Feron, P. H. M.; Versteeg, G. F., *Int. J. Greenhouse Gas Control* **2007,** *1* (1), 37-46.

51. Pinsent, B. R. W.; Pearson, L.; Roughton, F. J. W., *Trans. Faraday Soc.* **1956,** *52* (11), 1512-1520.

52. Liao, C. H.; Li, M. H., *Chem. Eng. Sci.* **2002,** *57* (21), 4569-4582.

53. Horng, S. Y.; Li, M. H., *Ind. Eng. Chem. Res.* **2002,** *41* (2), 257-266.

54. Blandamer, M. J.; Engberts, J.; Gleeson, P. T.; Reis, J. C. R., *Chem. Soc. Rev.* **2005,** *34* (5), 440-458.

55. Debye, P.; Huckel, E., *Physikalische Zeitschrift* **1923,** *24*, 185-206.

List of Figures

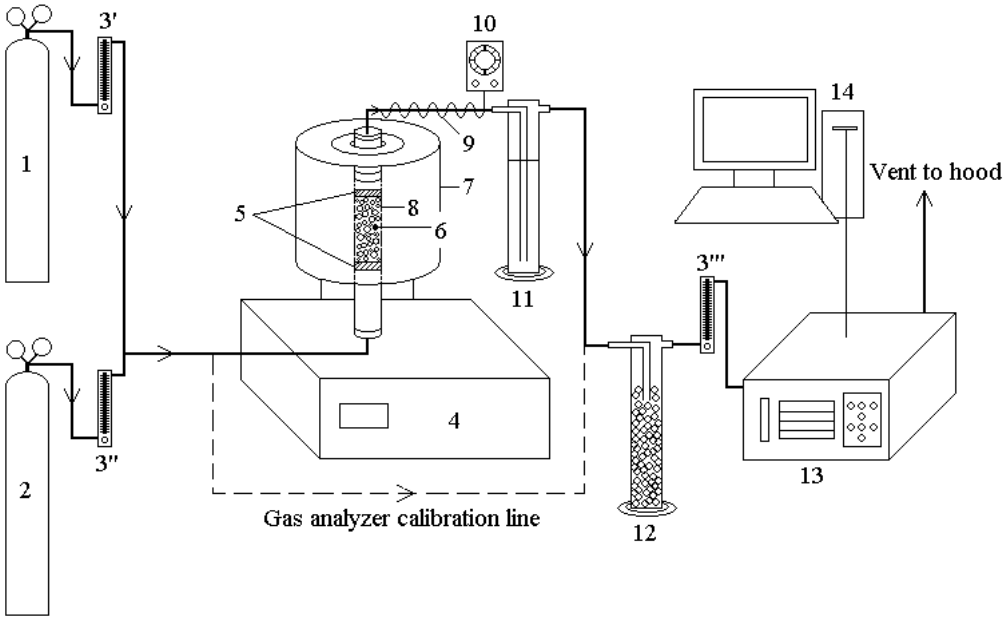
1
2
3'
3''
3'''
4
5
6
7
8
9
10
11
12
13
14
Vent to hood
Gas analyzer calibration line

Figure 1

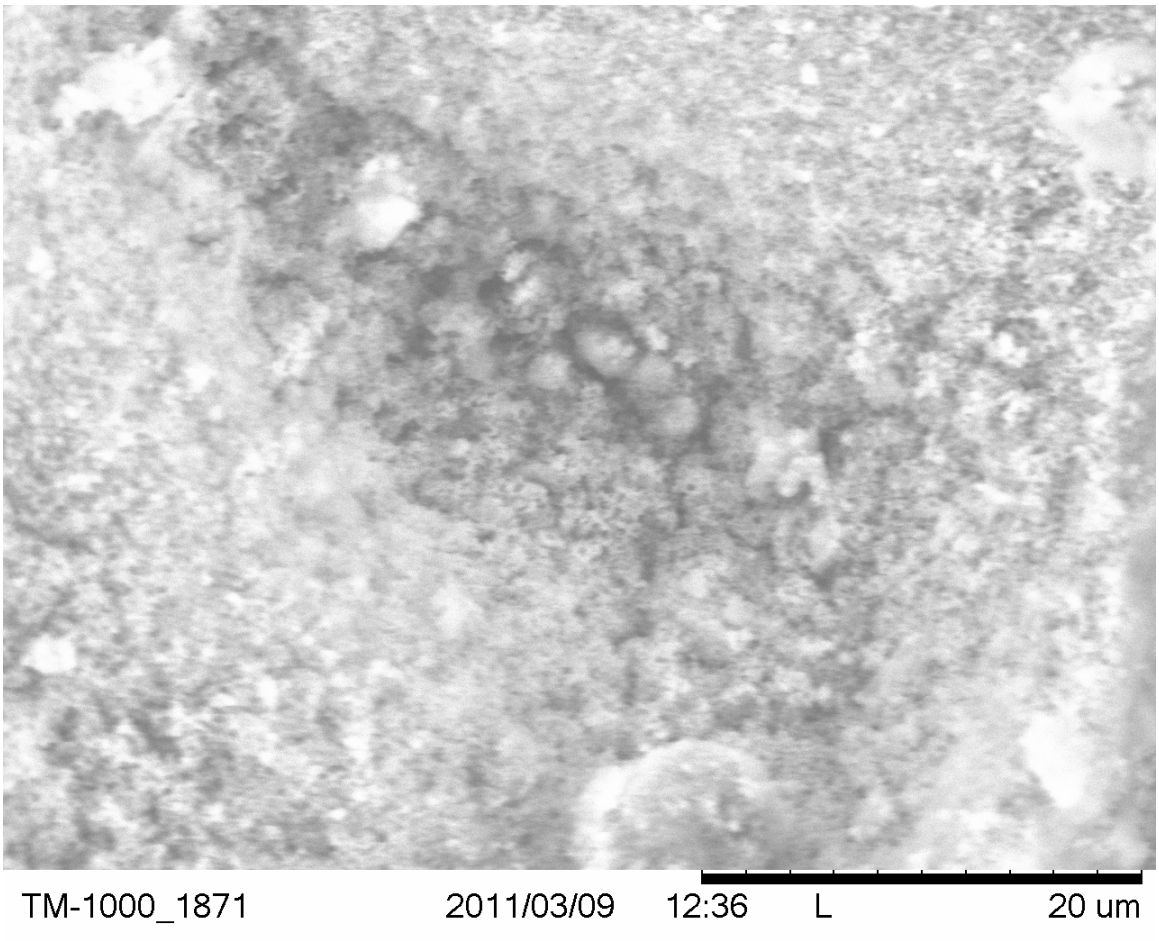

Figure 2

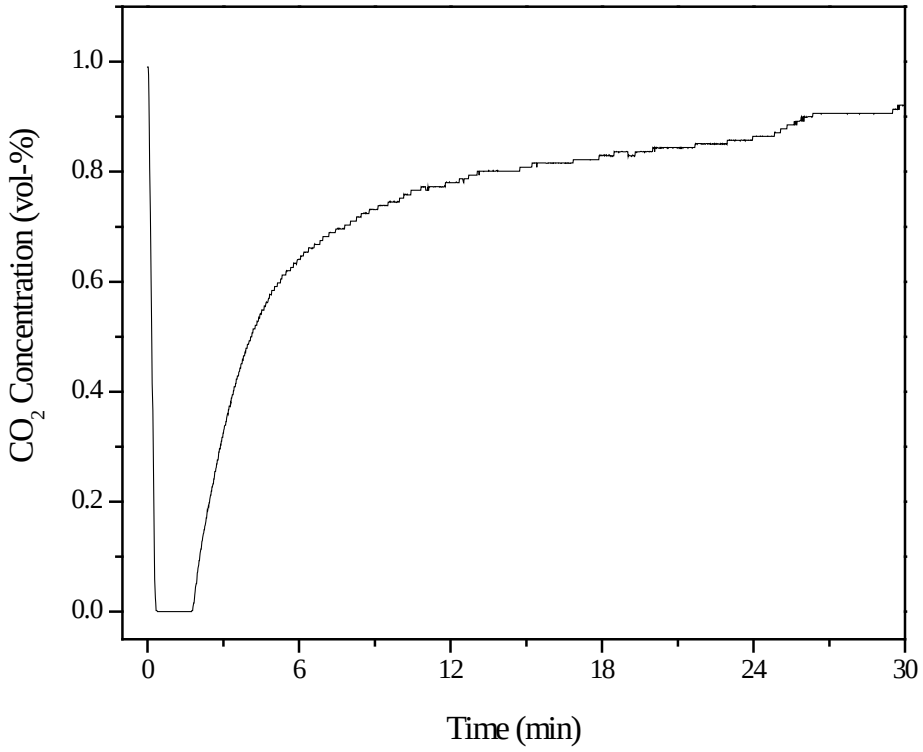

Figure 3

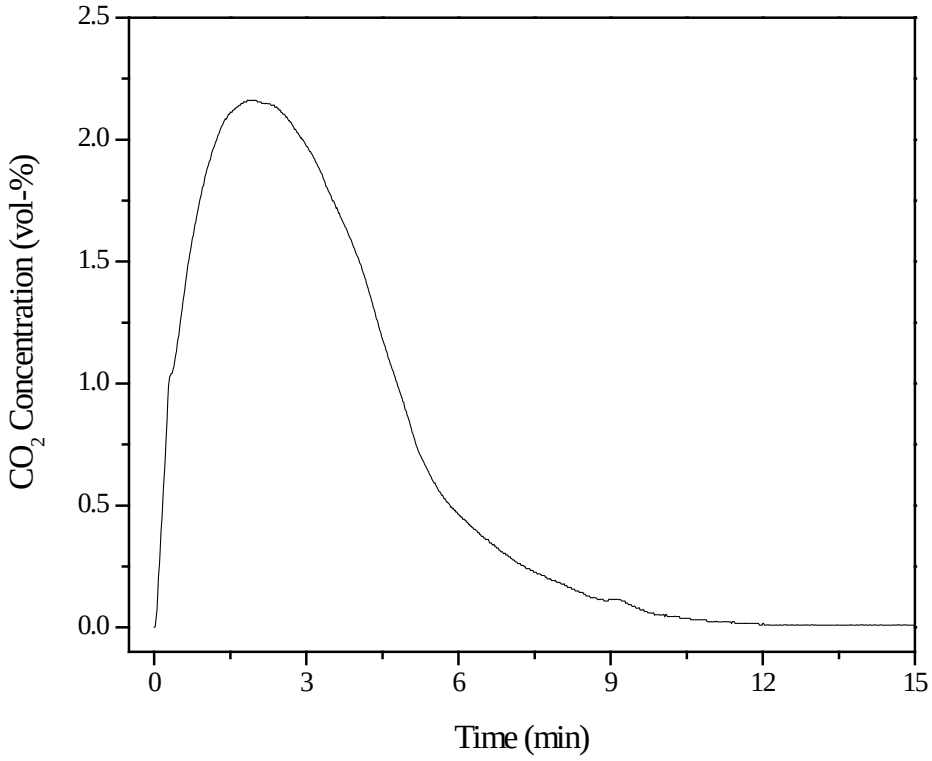

Figure 4

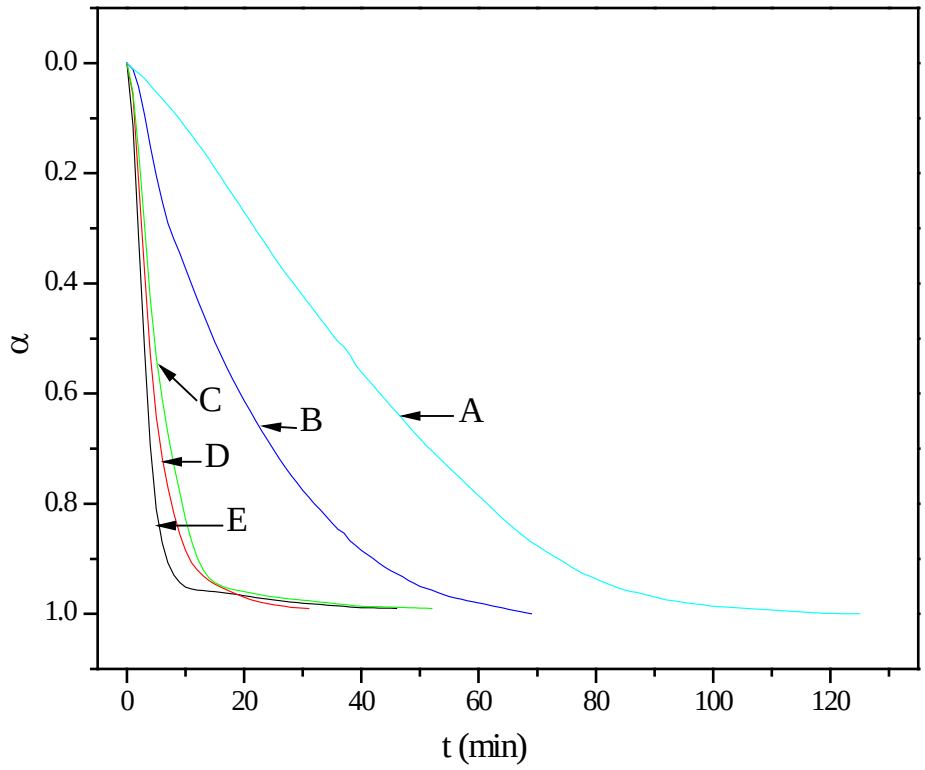

Figure 5

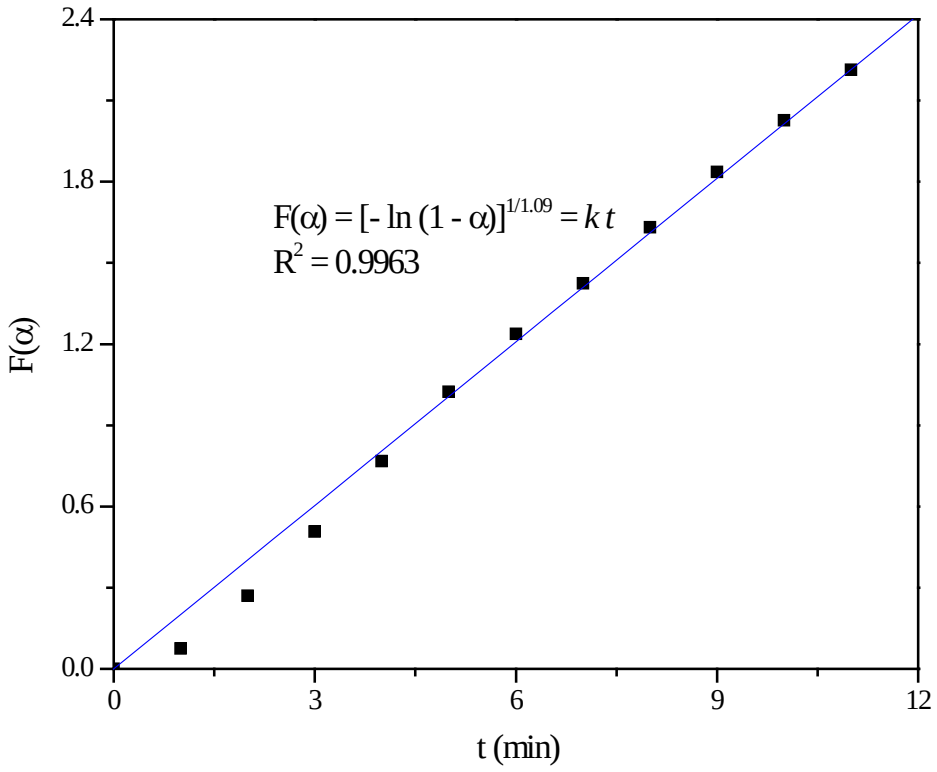

Figure 6

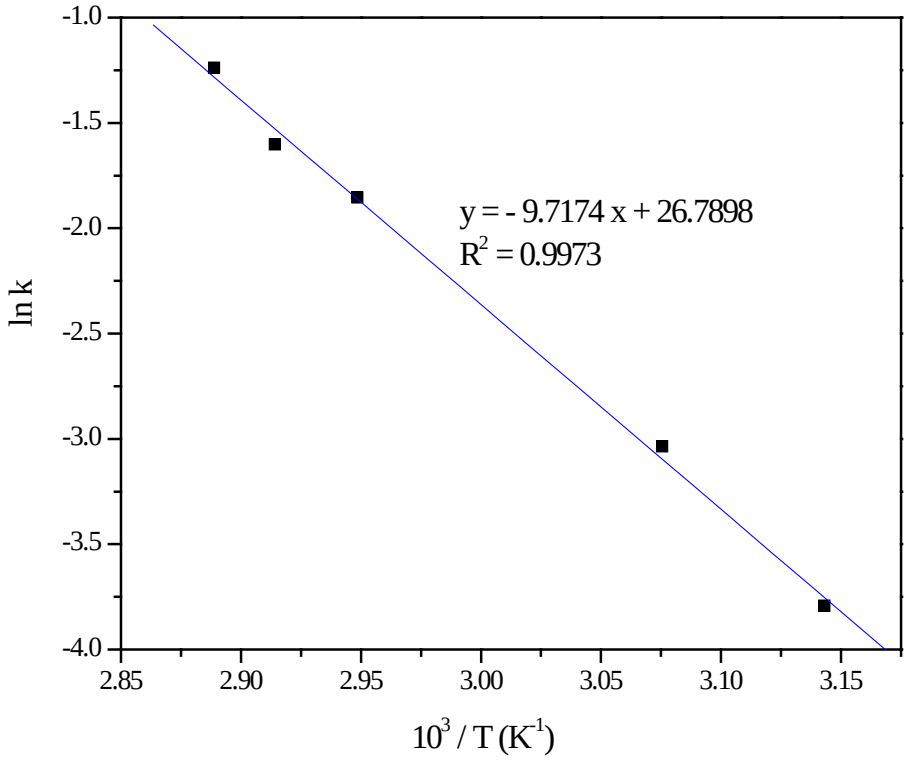
-1.0
-1.5
-2.0
-2.5
-3.0
-3.5
-4.0
ln k
2.85
2.90
2.95
3.00
3.05
3.10
3.15
y = - 9.7174 x + 26.7898
R2 = 0.9973
10^3 / T (K^-1)

Figure 7

List of Tables

Table 1

Temp. (℃)	$F(\alpha) = [-\ln(1-\alpha)]^{1/m}$			$F(\alpha) = 1-(1-\alpha)^{1/n}$		
	m	k (min^{-1})	r^2	n	k (min^{-1})	r^2
45.0	1.32	0.02319	0.9952	1.53	0.01101	0.9997
52.0	1.16	0.04800	0.9990	4.06	0.01022	0.9996
66.0	1.29	0.1564	0.9994	4.39	0.03507	0.9988
70.0	1.09	0.2014	0.9982	8.17	0.02445	0.9975
73.0	1.22	0.2897	0.9968	3.26	0.08030	0.9947

Table 2. Kinetic models of CO_2 desorption with and without presence of water[46]

With water $2RNH_2 + CO_2 + H_2O \xleftrightarrow{k_{R1},k_{-R1}} [RNH_3^+HCO_3]$ (R1)		Without water $2RNH_2 + CO_2 \xleftrightarrow{k_{R2},k_{-R2}} [RNH_3^+RNHCOO^-]$ (R2)	
E_a (kJ/mol)	n_i (reaction order)	E_a (kJ/mol)	n_i (reaction order)
114.25	$n_{RNH_3^+} = 1$ $n_{HCO_3^-} = 1$ $n_{H_2O} = -1$	102.74	$n_{RNH_3^+} = 1$ $n_{RNHCOO^-} = 1$ n_{H_2O}, not applicable